POLYMERS

Polymerization of a divalent/tetravalent metal-storing atom-mimicking dendrimer

Ken Albrecht,[1] Yuki Hirabayashi,[1] Masaya Otake,[1] Shin Mendori,[1] Yuta Tobari,[1] Yasuo Azuma,[2] Yutaka Majima,[2] Kimihisa Yamamoto[1]*

The phenylazomethine dendrimer (DPA) has a layer-by-layer electron density gradient that is an analog of the Bohr atom (atom mimicry). In combination with electron pair mimicry, the polymerization of this atom-mimicking dendrimer was achieved. The valency of the mimicked atom was controlled by changing the chemical structure of the dendrimer. By mimicking a divalent atom, a one-dimensional (1D) polymer was obtained, and by using a planar tetravalent atom mimic, a 2D polymer was obtained. These poly(dendrimer) polymers could store Lewis acids ($SnCl_2$) in their unoccupied orbitals, thus indicating that these poly(dendrimer) polymers consist of a series of nanocontainers.

INTRODUCTION

The (atomic) handling of nano-objects, that is, connecting macromolecules or nanoparticles with definite "valency" and "direction," is currently being pursued in the field of nanotechnology. At present, the controlled surface modification of particles (*1*–*6*) and the controlled placement of cross-linking (coordination) sites (*7*–*12*) are two approaches to handling such nano-objects. The development of "atom mimicry" (*10*, *13*, *14*) by containing various nano-objects in a narrow space appears to be a promising approach to expanding the frontiers to create architectures with the appropriate containers that allow the placement of objects into a framework.

Recently, the layer-by-layer, periodically-branched structure of the dendrimer has been attracting attention because of atom mimicry (*13*, *14*), with each dendrimer generation level resembling the traditional Bohr atomic orbital. However, each layer of the dendrimer generally has a different environment. Usually, this difference is unclear in that the difference in the coordination constant of each layer in a dendritic ligand cannot be detected (*15*). In contrast, some dendrimers have a clear electron density gradient in their backbone (*16*). A dendritic ligand with this electron density gradient shows a layer-by-layer stepwise coordination (*17*, *18*), and one of these is the phenylazomethine dendrimer (DPA) (*19*–*22*). DPA is a Schiff base dendritic ligand that coordinates to Lewis acids in a radial stepwise fashion. This behavior is an analog of filling the atomic orbital with electrons, and DPA definitely shows atom mimicry (Fig. 1). We now report the first examples of the one-dimensional (1D) and two-dimensional (2D) polymers of DPA by selectively cross-linking the innermost layer (first orbital) of DPA, which is the first "polymer of atom mimicry." This polymer can also store other objects in the inner space of the DPA. Therefore, this feature will provide a new method to locate nano-objects using the polymer as a template.

RESULTS

Design of the linker

To cross-link DPA, a rod with two Lewis acids at the periphery is necessary. The rod is required to be rigid to prevent the two Lewis acids from one rod from coordinating to one dendrimer, and the Lewis acid should be able to synthetically connect to the rod. Therefore, the combination of the phenylene ethynylene backbone and triphenylmethylium (TPM) cation (Lewis acid) (*23*) was selected as the linker, which is an analog of the covalent electron pair (Fig. 1). The length of the linker was designed to properly link each dendrimer in a molecular model (fig. S1).

The linker molecule was synthesized by a combination of the Sonogashira coupling and the deprotection of the trimethylsilyl (TMS) group, which is a typical route to synthesize oligo(phenylene ethynylenes) (*24*, *25*). The triphenyl methanol unit was introduced to the periphery by Sonogashira coupling. The OH group was converted into chlorine and, finally, reacted with $AgBF_4$ to obtain the dication linker (scheme S1 to S9, figs. S2 to S15).

Confirming the formation of the polymer by UV-vis titration

The stepwise coordination of a Lewis acid to DPA can be traced by ultraviolet-visible (UV-vis) titration; that is, the sequential shift of the isosbestic point that corresponds to the coordination to each layer can be observed upon titration (*17*–*22*). However, titrating more than 1 eq of a linker with DPA will cause a complex network structure that is difficult to evaluate. Therefore, the complexation of the linker molecule to the innermost layer was confirmed by additional titration of $SnCl_2$ (a Lewis acid that has a lower binding constant to DPA compared to TPM) (*23*) to a 1:1 mixture of DPAG4 and the linker (Fig. 2A). First, the addition of 1 eq of the linker (2 eq of cation versus one dendrimer) caused an increase in the absorbance at 350 to 450 nm, and notably, the absorption of the linker cation (at 578 nm, $\varepsilon = 5.9 \times 10^4\ M^{-1}\ cm^{-1}$) disappeared. This indicated the coordination of the linker to DPAG4. Subsequently, $SnCl_2$ was titrated into the solution. Upon addition of $SnCl_2$, the absorption around 450 nm increased, and the absorption around 300 nm decreased. Careful observation revealed the existence of three isosbestic points, and the amounts of $SnCl_2$ that were necessary for the shift were 4, 8, and 16 eq, amounts which correspond to the number of imine sites of the second, third, and fourth layers of DPAG4, respectively, and agree with the stepwise complexation from the second layer to the fourth layer of DPAG4. Consequently, the UV-vis titration shows that the linker is coordinating to the innermost layer of the DPA, forming a coordination polymer, and the DPA polymer can store other Lewis acids. The same UV-vis titration was also performed for a four-substituted DPA [ZnPG4 (zinc porphyrin core DPA) (*26*); figs. S16 and S17]. Similar to a two-substituted DPA, three isosbestic points

[1]Laboratory for Chemistry and Life Science, Tokyo Institute of Technology, 4259 Nagatsuta Midori-ku, Yokohama 226-8503, Japan. [2]Laboratory for Materials and Structures, Tokyo Institute of Technology, 4259 Nagatsuta Midori-ku, Yokohama 226-8503, Japan.
*Corresponding author. Email: yamamoto@res.titech.ac.jp

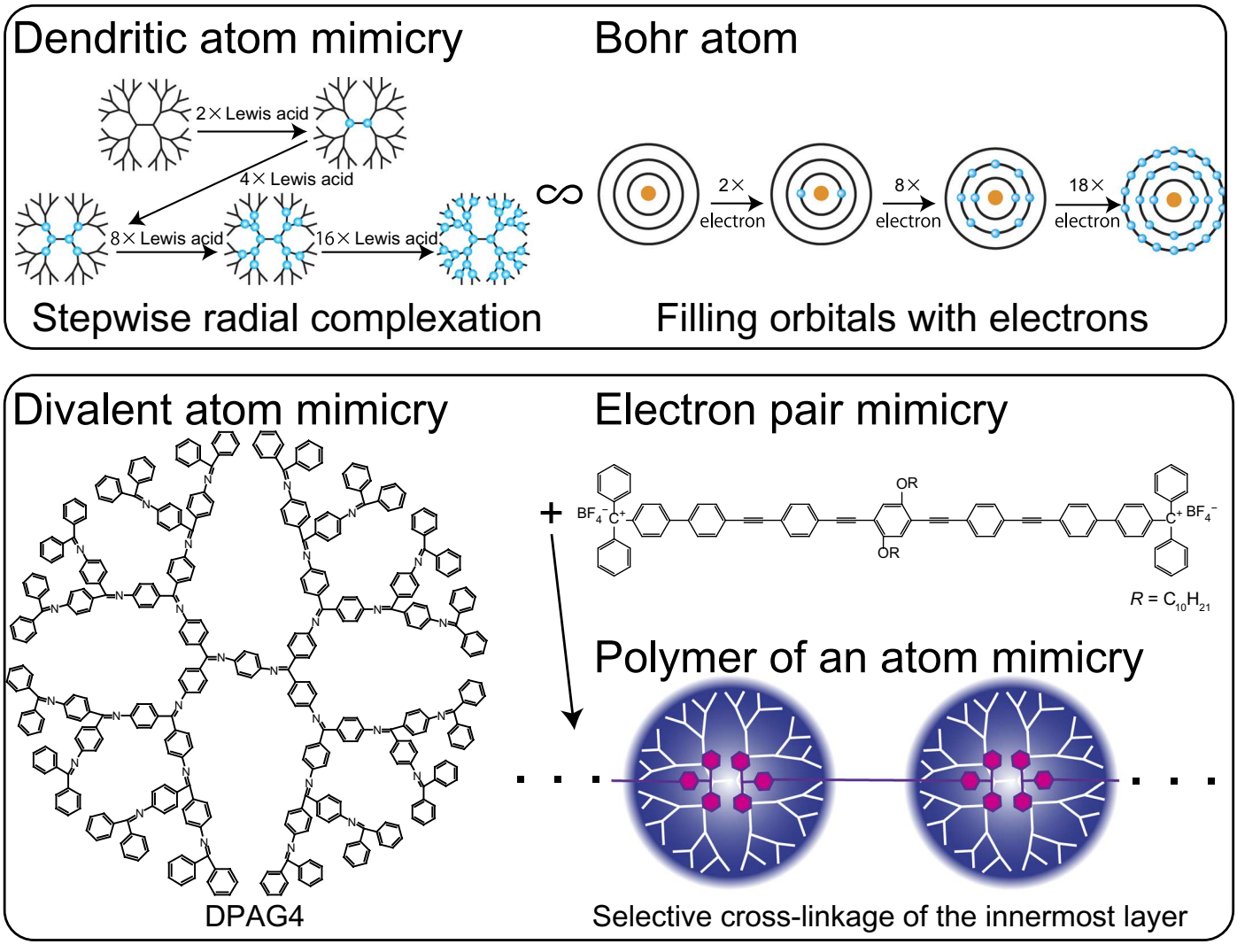

Fig. 1. Exhibition of DPA as an atom mimicry and its polymerization. (**Top**) Comparison of the DPA and Bohr atom model. (**Bottom**) Polymerization of dendritic atom mimicry using a cross-linking molecule (electron pair mimicry).

that correspond to the coordination of $SnCl_2$ to the second, third, and fourth layers of the dendrimer were observed. This result confirms that the coordination of the linker occurs at the innermost layer of the dendrimer, and that $SnCl_2$ can be stored in the dendrimer even if the core (valency) of the dendrimer changes.

Light-scattering measurements of the polymer

The formation of a linear supramolecular polymer (*27*–*33*) was confirmed by light-scattering measurements. The multiangle light-scattering (MALS) measurement and the Zimm plot (fig. S18A) revealed that the polymer has a molecular weight of (6.8 ± 0.6) × 10^5 g/mol that corresponds to a degree of polymerization (DP) of 98 and a radius of gyration (Rg) of 101 ± 28 nm. The theoretical DP (*34*, *35*) calculated from the binding constant of DPAG1 and the linker (1.0×10^7 M^{-1}; fig. S19) is 108, which is in agreement with the observed value (*23*). Additionally, the Kratky plot of the MALS measurement had a linear slope that suggests formation of an anisotropic chain (fig. S20) (*36*–*39*). The dynamic light-scattering (DLS) measurement at a similar concentration (fig. S21) showed a hydrodynamic radius (Rh) of 76 nm; thus, the Rg/Rh value was determined to be 1.33. This indicates that the supramolecular polymer has an anisotropic structure with some flexibility (worm-like chain) (*40*). The MALS measurement was also performed for the 1D polymer with 12 eq of $SnCl_2$ per dendrimer. This result shows the existence of a linear polymer with a molecular weight of (4.6 ± 0.9) × 10^5 g/mol that corresponds to a DP of 52 and an Rg of 95.4 ± 17 nm. The big difference in the second virial coefficient compared to the polymer without $SnCl_2$ indicates that the interpolymer interaction decreased as a result of storing $SnCl_2$ (fig. S18B). The decrease in DP was observed, but Rg was identical. This probably suggests that the linearity of the polymer had increased. The DLS measurement (fig. S22) showed an Rh of 30 nm; thus, the Rg/Rh value was determined to be 3.18. This high Rg/Rh value also supports the result of the MALS measurement; that is, the polymer with $SnCl_2$ takes a more rigid, rod-like conformation compared to the polymer without $SnCl_2$. This result indicates that the 1D supramolecular polymer can

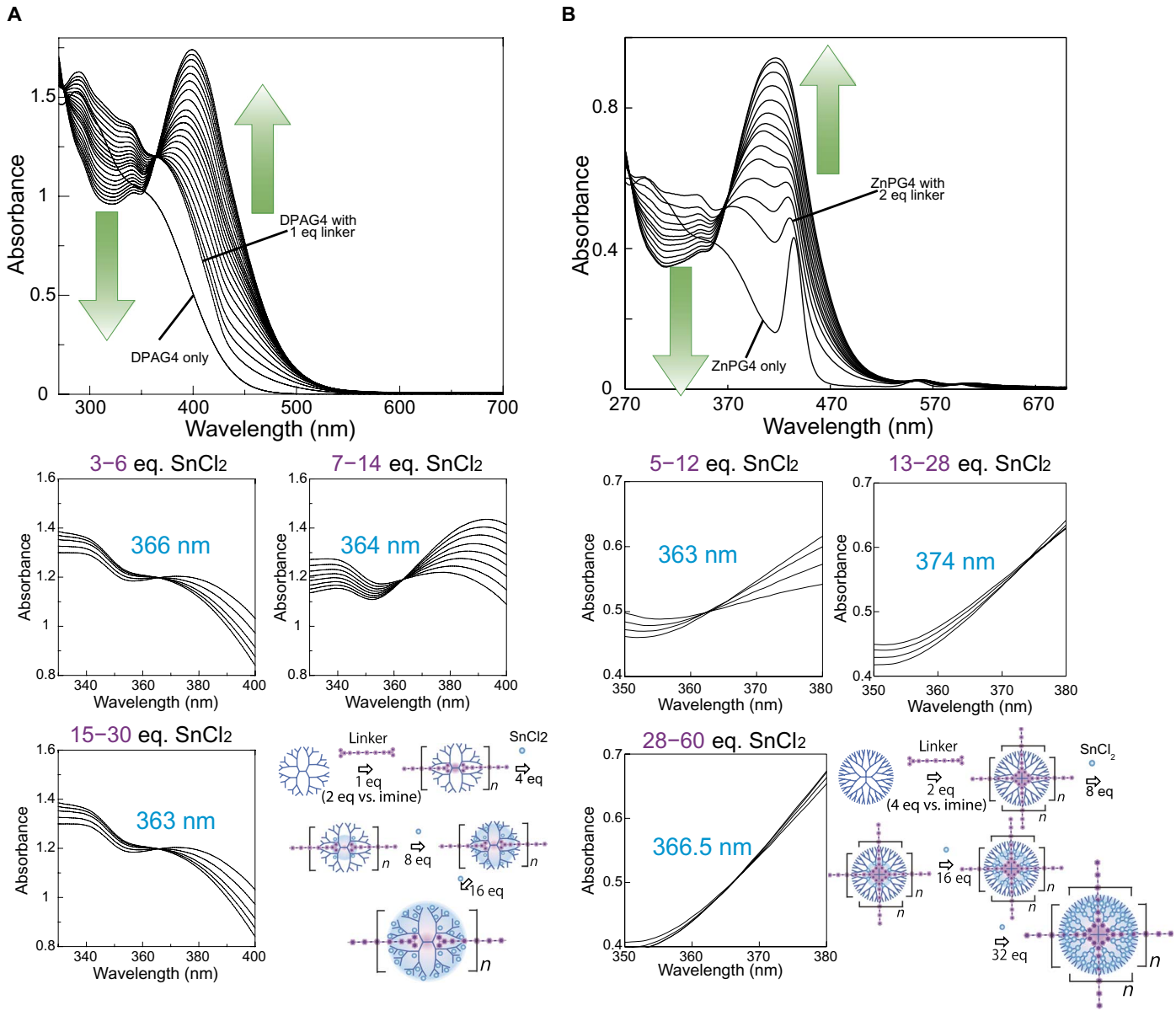

Fig. 2. UV-vis spectra during titration. (**A**) DPAG4 during the addition of 1 eq of the linker followed by 28 eq of $SnCl_2$ (the solvent is dichloromethane/acetonitrile, 1:1) and (**B**) ZnPG4 during the addition of 2 eq of the linker followed by 56 eq of $SnCl_2$ (the solvent is dichloromethane/acetonitrile, 1:1).

successfully store $SnCl_2$. Accordingly, a light-scattering study revealed the formation of a linear polymer. This verifies the cross-linking of the innermost layer because otherwise, if the linkage occurred in other layers, it would form an isotropic aggregate.

Microscopy of the polymer

The structure of the supramolecular polymer was also analyzed by microscopy. The solution of the 1:1 mixture of DPAG4 and the linker was drop-cast onto highly ordered pyrolytic graphite (HOPG). Fibrous objects with a height of one or two dendrimers were observed in the atomic force microscopy (AFM) image (Fig. 3 and fig. S23). The width was greater than one dendrimer plus the width of the probe, which can be attributed to the bundling of the polymers. Also, a single chain was observed, but this structure could not be seen if the linker and dendrimer were mixed at a 0.5:1 composition (figs. S24 and S25). Further examination by scanning tunneling microscopy (STM) revealed the existence of a single chain with a width of 3 nm, which corresponds to the short axis of the dendrimer. The observed polymer also had a periodic structure that can be attributed to the dendrimer unit (Fig. 3 and figs. S26 and S27). The molecular model of the dendrimer with a linker (figs. S28 and S29) indicates that the supramolecular polymer can have several conformations. The STM image shows some bend (fig. S30), but overall, the polymer chain shows a linear, highly anisotropic structure.

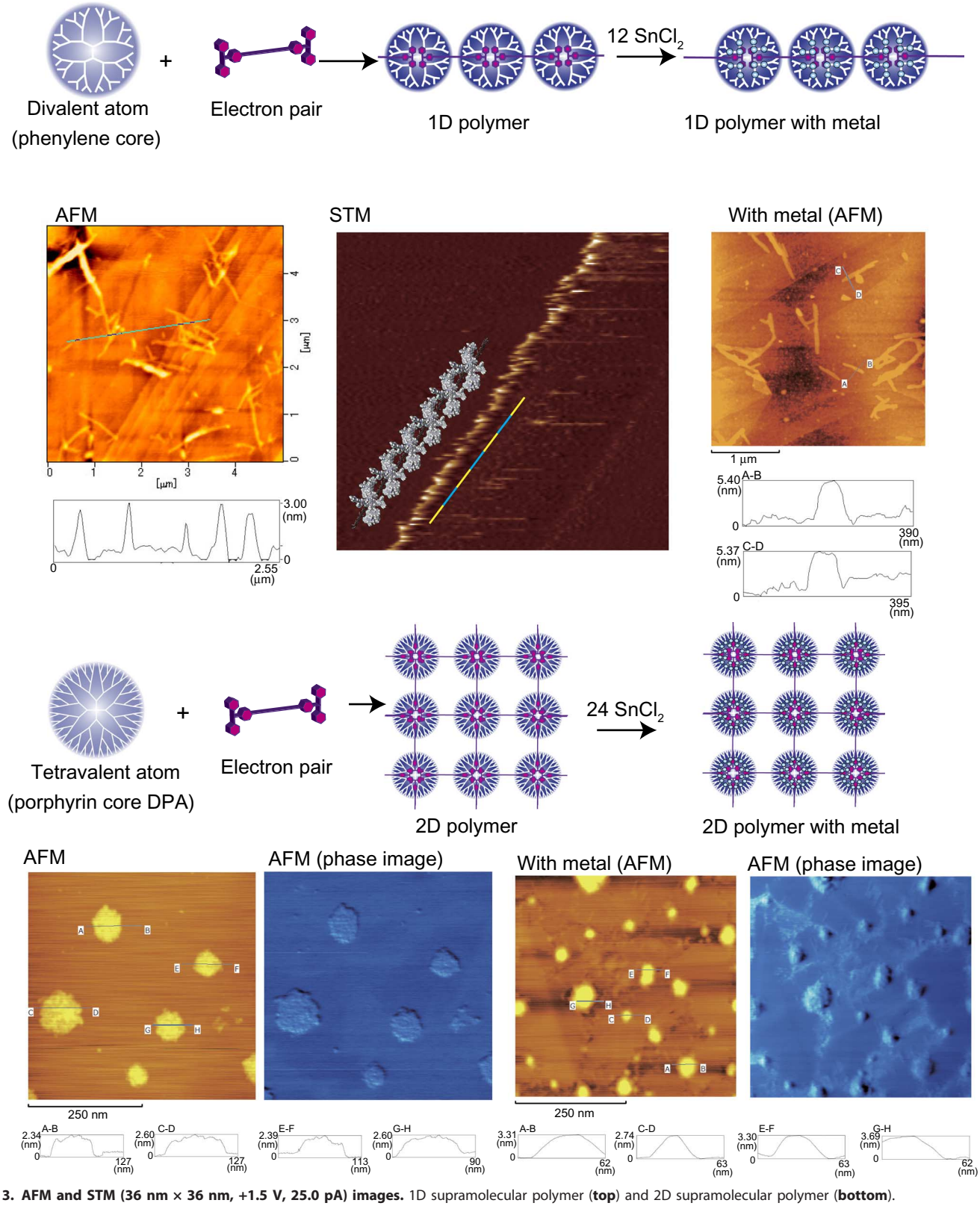

Fig. 3. AFM and STM (36 nm × 36 nm, +1.5 V, 25.0 pA) images. 1D supramolecular polymer (**top**) and 2D supramolecular polymer (**bottom**).

2D polymer

The valency of the dendrimer can be easily controlled by changing the core. A planar four-substituted porphyrin core dendrimer (ZnPG4; fig. S16) is expected to have a valency of "four" and form a 2D supramolecular polymer in the presence of 2 eq of the linker. The 1:2 mixture of ZnPG4 and the linker was drop-cast onto HOPG. The AFM image showed the formation of a sheet with a height of about 2 to 3 nm. This structure cannot be observed with only the dendrimer (fig. S31) and with an excess (6 eq) amount of the linker (larger aggregates were observed; fig. S32). The height of the sheet corresponds to the flattened dendrimer with the porphyrin ring parallel to the HOPG substrate (fig. S17). Therefore, this is attributed to a 2D polymer sheet (*41*–*44*). The DLS analysis of the solution showed an Rh of 32 nm. The slope of the linker equivalent versus the hydrodynamic radii plot showed a decrease when more than 2 eq of the linker was added (fig. S33). This indicates that the growing dimension of the supramolecular polymer increased by increasing the amount of the linker. The supramolecular polymer grows two-dimensionally until the first layer of the dendrimer is occupied and then starts to grow three-dimensionally because the second-layer imine sites have a greater steric hindrance and a diverse configuration. The AFM image of the dendrimer with 6 eq of the linker also supports this (fig. S32); that is, it showed aggregates that are higher than the 2D sheet (the height and the distribution were much larger than the proper 2D sheet; see fig. S32). The MALS analysis was also provided (fig. S34). The Rg of the supramolecular polymer was much lower than that of the linear polymer at a similar concentration (1D, 101 ± 28 nm; 2D, 26 ± 42 nm), but the determined absolute molecular weight was higher [1D, (6.8 ± 0.6) × 10^5 g/mol; 2D, (2.7 ± 0.4) × 10^6 g/mol]. This indicates that the supramolecular polymer of the tetravalent dendrimer is denser than the divalent dendrimer polymer, which means that the supramolecular polymer of the tetravalent dendrimer has a higher dimension of growth than the 1D polymer. Furthermore, the Rg/Rh value was 0.8 for the 2D polymer. This supports the fact that the dimension of the supramolecular polymer is between 1D and 3D. Overall, these data prove that the valency control of the dendrimer can control the structure of the supramolecular polymer.

Metal accumulation to the polymer

As demonstrated in Fig. 2, the DPA-linker supramolecular polymer has extra coordination sites (unoccupied orbitals) that can be used to accumulate various Lewis acids. The AFM image of the linear polymer with 12 eq of $SnCl_2$ per DPAG4-linker and 28 eq of $SnCl_2$ per ZnPG4-linker showed results very similar to those of the polymer without $SnCl_2$ (Fig. 3). The accumulation of 12 eq of $PtCl_4$ (heavy atom) per DPAG4 has also allowed us to obtain scanning transmission electron microscopy (STEM) images of the network of the linear polymer (fig. S35). These data indicate that the DPA polymer can store metal salts (Lewis acids) and can be used as a chain of nanocontainers.

DISCUSSION

A supramolecular polymer that consists of atom mimicry (DPA) and electron pair mimicry (linker molecule) was developed. The valency of the DPA could be easily controlled by changing the core substitution number, and as a result, the formation of 1D and 2D polymers was confirmed. Therefore, this system will lead to the construction of various supramolecular structures by changing the dendrimer (valency) and designing the appropriate linker. Additionally, the DPA exhibiting atom mimicry could store other Lewis acids in its outer orbitals. This means that DPA can give valency and direction to the stored molecules (or nanoparticles that are formed in DPA). This describes a new aspect of atom mimicry, that is, the use of atom-mimicking nanocontainers to give atomicity to various molecules that can be stored in the container. Thus, the metal-storing supramolecular polymer provides the possibility of constructing arrays of zero valence (*20*, *21*) or oxide (*19*) nanoparticles on a substrate. The geometry and pitch can be controlled by the design of the dendrimer and the linker and are potentially applicable to plasmonics (after seed-mediated growth) and nanoelectrode grids (which are also useful as electrocatalysts).

MATERIALS AND METHODS

Chemicals

DPAG4 (*45*) and ZnPG4 (fig. S16) (*26*) were synthesized according to previously described methods in the literature. Chemicals were purchased from Kanto Kagaku Co. Ltd., Tokyo Chemical Industry Co. Ltd., Wako Pure Chemical Industries Ltd., or Aldrich and used without further purification (solvents for the UV-vis titration and reactions were of dehydrated grade). The silica gel for column chromatography was of neutral grade (Kanto Kagaku Co. Ltd.).

General

The nuclear magnetic resonance (NMR) spectra were obtained using a Bruker AVANCE III 400 (400 MHz). The ^{1}H NMR and ^{13}C NMR spectra were measured with TMS as the internal standard. The matrix-assisted laser desorption/ionization–time-of-flight mass spectrometry data were obtained using a Shimadzu Kratos AXIMA-CFR Plus in the linear positive ion mode. Dithranol was used as the matrix. The UV-vis spectra were recorded using a Shimadzu UV-2700 with a quartz cell (optical length, 1 cm) at 20°C in a glove box. The elemental analysis was performed at the Center for Advanced Materials Analysis, Technical Department, Tokyo Institute of Technology. The molecular models were calculated with SCIGRESS v2.1.0 (Fujitsu) using the MM/AM1 MOZYME method and with Gaussian 09, Revision C.01 (*46*) on the nodes of a supercomputer (TSUBAME2, Tokyo Institute of Technology). A preparative scale gel permeation chromatograph, LC-908 (Japan Analytical Industry Co. Ltd.), was used to isolate each compound with chloroform as the eluent.

Multiangle light scattering

MALS was performed using a DAWN HELEOS II spectrometer in batch mode with a 690-nm laser (Wyatt Technology Corp.) after filtering the dendrimer and linker solution with a hydrophobic membrane filter (pore size, 0.5 μm). The refractive index increment (*dn*/*dc*) was determined using an Optilab T-rEX Wyatt Interferometric Refractometer and was found to be 0.049 ml g^{-1}. The concentrations were 0.6, 0.8, and 1.0 mg/ml.

Dynamic light scattering

The DynaPro NanoStar with a Temperature-Controlled MicroSampler (Wyatt Technology Corp.) was used for DLS measurements after filtering the dendrimer and linker solution with a hydrophobic membrane filter (pore size, 0.5 μm). The concentration was 0.8 mg/ml.

Atomic force microscopy

AFM was performed with a commercial atomic force microscope (Shimadzu WET-SPM FM-AFM and SII SPA400) operating in direct

force mode using rectangular silicon cantilevers (NanoWorld; 125 μm long, 30 μm wide, 4 μm thick) with an integrated tip, a normal spring constant of 42 N/m, and a resonance frequency of 320 kHz.

Scanning tunneling microscopy

Ultrahigh-vacuum (UHV) STM was conducted using a JSPM-4500 (JEOL). All STM observations and scanning tunneling spectroscopy measurements were conducted using a UHV scanning tunneling microscope at room temperature. A tungsten tip, which was prepared by electrochemically etching a tungsten wire, was used as an STM tip. All STM images were taken in constant-current mode at a set point current of 25 pA and a bias voltage of 1.5 V.

Scanning transmission electron microscopy

STEM images were obtained via a transmission electron microscope (JEM-2100F, JEOL) using the high-angle annular dark-field method. The samples were deposited on a carbon film with a Cu mesh (Super Ultra-High Resolution Carbon film with Cu grid; Okenshoji Co.). Sample preparation conditions, synthesis, and identification data are described in the Supplementary Materials.

SUPPLEMENTARY MATERIALS

Supplementary material for this article is available at http://advances.sciencemag.org/cgi/content/full/2/12/e1601414/DC1

fig. S1. Molecular models of DPA G4 and linker molecule.
fig. S2. ^{1}H NMR spectrum (400 MHz, $CDCl_3$, 302 K) of **2.**
fig. S3. ^{13}C NMR spectrum (100 MHz, $CDCl_3$, 302 K) of **2.**
fig. S4. ^{1}H NMR spectrum (400 MHz, $CDCl_3$, 302 K) of **3.**
fig. S5. ^{13}C NMR spectrum (100 MHz, $CDCl_3$, 302 K) of **3.**
fig. S6. ^{1}H NMR spectrum (400 MHz, $CDCl_3$, 302 K) of **4.**
fig. S7. ^{13}C NMR spectrum (100 MHz, $CDCl_3$, 302 K) of **4.**
fig. S8. ^{1}H NMR spectrum (400 MHz, $CDCl_3$, 302 K) of **5.**
fig. S9. ^{13}C NMR spectrum (100 MHz, $CDCl_3$, 302 K) of **5.**
fig. S10. ^{1}H NMR spectrum (400 MHz, $CDCl_3$, 302 K) of **6.**
fig. S11. ^{13}C NMR spectrum (100 MHz, $CDCl_3$, 302 K) of **6.**
fig. S12. ^{1}H NMR spectrum (400 MHz, $CDCl_3$, 303 K) of **7.**
fig. S13. ^{13}C NMR spectrum (100 MHz, $CDCl_3$, 303 K) of **7.**
fig. S14. ^{1}H NMR spectrum (400 MHz, dehydrated $CDCl_3$, 303 K) of **8.**
fig. S15. ^{13}C NMR spectrum (100 MHz, $CDCl_3$, 302 K) of **8** and **7**.
fig. S16. Structure of ZnPG4.
fig. S17. Molecular model of ZnPG4.
fig. S18. MALS analysis of 1D supramolecular polymer with and without 12 eq $SnCl_2$.
fig. S19. UV-vis spectra of a linker molecule during the addition of DPAG1.
fig. S20. MALS analysis of 1D supramolecular polymer (Kratky plot at 0.8 mg ml^{-1}).
fig. S21. DLS analysis of the 1D supramolecular polymer.
fig. S22. DLS analysis of the 1D supramolecular polymer with 12 eq of $SnCl_2$.
fig. S23. AFM images of the 1D supramolecular polymer.
fig. S24. AFM image of DPAG4 and 0.5 eq linker.
fig. S25. AFM phase image of the 1D supramolecular polymer.
fig. S26. Enlarged STM image of 1D supramolecular polymer with a molecular model of DPA G4.
fig. S27. 3D STM topograph image of the 1D supramolecular polymer with a molecular model of the polymer.
fig. S28. Molecular model and structure of DPAG0 and TPM cation.
fig. S29. Representative molecular model of DPAG1 and two linker molecules.
fig. S30. STM image of 1D supramolecular polymer with molecular models.
fig. S31. Representative AFM topological image of ZnPG4.
fig. S32. Representative AFM topological images of ZnPG4 with 6eq of the linker.
fig. S33. DLS analysis of ZnPG4 with linker in several ratios.
fig. S34. MALS analysis of 2D supramolecular polymer (ZnPG4 with 2 eq of the linker; Zimm plot).
fig. S35. STEM images of the 2D supramolecular polymer.
scheme S1. Synthesis of **1.**
scheme S2. Synthesis of **2.**
scheme S3. Synthesis of **3.**
scheme S4. Synthesis of **4.**
scheme S5. Synthesis of **5.**
scheme S6. Synthesis of **6.**
scheme S7. Synthesis of **7.**
scheme S8. Synthesis of **8.**
scheme S9. Synthesis of **9.**

REFERENCES AND NOTES

1. G. A. DeVries, M. Brunnbauer, Y. Hu, A. M. Jackson, B. Long, B. T. Neltner, O. Uzun, B. H. Wunsch, F. Stellacci, Divalent metal nanoparticles. *Science* **315**, 358–361 (2007).
2. H.-Y. Lee, S. H. R. Shin, A. M. Drews, A. M. Chirsan, S. A. Lewis, K. J. M. Bishop, Self-assembly of nanoparticle amphiphiles with adaptive surface chemistry. *ACS Nano* **8**, 9979–9987 (2014).
3. K. Liu, Z. Nie, N. Zhao, W. Li, M. Rubinstein, E. Kumacheva, Step-growth polymerization of inorganic nanoparticles. *Science* **329**, 197–200 (2010).
4. J. Wei, N. Schaeffer, M.-P. Pileni, Ligand exchange governs the crystal structures in binary nanocrystal superlattices. *J. Am. Chem. Soc.* **137**, 14773–14784 (2015).
5. B. Teschome, S. Facsko, K. V. Gothelf, A. Keller, Alignment of gold nanoparticle-decorated DNA origami nanotubes: Substrate prepatterning versus molecular combing. *Langmuir* **31**, 12823–12829 (2015).
6. D. Jishkariani, B. T. Diroll, M. Cargnello, D. R. Klein, L. A. Hough, C. B. Murray, B. Donnio, Dendron-mediated engineering of interparticle separation and self-assembly in dendronized gold nanoparticles superlattices. *J. Am. Chem. Soc.* **137**, 10728–10734 (2015).
7. L. J. Hill, N. E. Richey, Y. Sung, P. T. Dirlam, J. J. Griebel, E. Lavoie-Higgins, I.-B. Shim, N. Pinna, M.-G. Willinger, W. Vogel, J. J. Benkoski, K. Char, J. Pyun, Colloidal polymers from dipolar assembly of cobalt-tipped CdSe@CdS nanorods. *ACS Nano* **8**, 3272–3284 (2014).
8. Y. Wang, Y. Wang, D. R. Breed, V. N. Manoharan, L. Feng, A. D. Hollingsworth, M. Weck, D. J. Pine, Colloids with valence and specific directional bonding. *Nature* **491**, 51–55 (2012).
9. M. A. Olson, A. Coskun, R. Klajn, L. Fang, S. K. Dey, K. P. Browne, B. A. Grzybowski, J. F. Stoddart, Assembly of polygonal nanoparticle clusters directed by reversible noncovalent bonding interactions. *Nano Lett.* **9**, 3185–3190 (2009).
10. M. A. van Dongen, S. Vaidyanathan, M. M. B. Holl, PAMAM dendrimers as quantized building blocks for novel nanostructures. *Soft Matter* **9**, 11188–11196 (2013).
11. Z. Niu, S. Fang, X. Liu, J.-G. Ma, S. Ma, P. Cheng, Coordination-driven polymerization of supramolecular nanocages. *J. Am. Chem. Soc.* **137**, 14873–14876 (2015).
12. L. Chen, O. Chen, M. Wu, F. Jiang, M. Hong, Controllable coordination-driven self-assembly: From discrete metallocages to infinite cage-based frameworks. *Acc. Chem. Res.* **48**, 201–210 (2015).
13. D. A. Tomalia, S. N. Khanna, In quest of a systematic framework for unifying and defining nanoscience. *Mod. Phys. Lett. B* **28**, 1430002 (2014).
14. D. A. Tomalia, S. N. Khanna, A systematic framework and nanoperiodic concept for unifying nanoscience: Hard/soft nanoelements, superatoms, meta-atoms, new emerging properties, periodic property patterns, and predictive mendeleev-like nanoperiodic tables. *Chem. Rev.* **116**, 2705–2774 (2016).
15. D. Astruc, E. Boisselier, C. Ornelas, Dendrimers designed for functions: From physical, photophysical, and supramolecular properties to applications in sensing, catalysis, molecular electronics, photonics, and nanomedicine. *Chem. Rev.* **110**, 1857–1959 (2010).
16. K. Albrecht, K. Yamamoto, Dendritic structure having a potential gradient: New synthesis and properties of carbazole dendrimers. *J. Am. Chem. Soc.* **131**, 2244–2251 (2009).
17. K. Yamamoto, M. Higuchi, S. Shiki, M. Tsuruta, H. Chiba, Stepwise radial complexation of imine groups in phenylazomethine dendrimers. *Nature* **415**, 509–511 (2002).
18. M. Kathiresan, L. Walder, Shell-by-shell inside-out complexation of organic anions in flexible and rigid pyridinium dendrimers. *Macromolecules* **44**, 8563–8574 (2011).
19. N. Satoh, T. Nakashima, K. Kamikura, K. Yamamoto, Quantum size effect in TiO_2 nanoparticles prepared by finely controlled metal assembly on dendrimer templates. *Nat. Nanotechnol.* **3**, 106–111 (2008).
20. K. Yamamoto, T. Imaoka, W.-J. Chun, O. Enoki, H. Katoh, M. Takenaga, A. Sonoi, Size-specific catalytic activity of platinum clusters enhances oxygen reduction reactions. *Nat. Chem.* **1**, 397–402 (2009).
21. K. Yamamoto, T. Imaoka, Precision synthesis of subnanoparticles using dendrimers as a superatom synthesizer. *Acc. Chem. Res.* **47**, 1127–1136 (2014).
22. K. Albrecht, N. Sakane, K. Yamamoto, Stepwise radial complexation from the outer layer to the inner layer of the dendritic ligand: Phenylazomethine dendrimer with an inverted coordination sequence. *Chem. Commun.* **50**, 12177–12180 (2014).
23. Y. Ochi, A. Fujii, R. Nakajima, K. Yamamoto, Stepwise radial complexation of triphenylmethyliums on a phenylazomethine dendrimer for organic–metal hybrid assembly. *Macromolecules* **43**, 6570–6576 (2010).
24. F. Pertici, N. Varga, A. van Duijn, M. Rey-Carrizo, A. Bernardi, R. J. Pieters, Efficient synthesis of phenylene-ethynylene rods and their use as rigid spacers in divalent inhibitors. *Beilstein J. Org. Chem.* **9**, 215–222 (2013).

25. C. Xue, F.-T. Luo, Rapid syntheses of oligo(*p*-phenyleneethynylene)s via iterative convergent approach. *Tetrahedron* **60**, 6285–6294 (2004).
26. T. Imaoka, R. Tanaka, S. Arimoto, M. Sakai, M. Fujii, K. Yamamoto, Probing stepwise complexation in phenylazomethine dendrimers by a metallo-porphyrin core. *J. Am. Chem. Soc.* **127**, 13896–13905 (2005).
27. A. W. Bosman, R. P. Sijbesma, E. W. Meijer, Supramolecular polymers at work. *Mater. Today* **7**, 34–39 (2004).
28. J.-M. Lehn, Supramolecular polymer chemistry—Scope and perspectives. *Polym. Int.* **51**, 825–839 (2002).
29. Y. Liu, Z. Wang, X. Zhang, Characterization of supramolecular polymers. *Chem. Soc. Rev.* **41**, 5922–5932 (2012).
30. T. Aida, E. W. Meijer, S. I. Stupp, Functional supramolecular polymers. *Science* **335**, 813–817 (2012).
31. H.-J. Sun, S. Zhang, V. Percec, From structure to function via complex supramolecular dendrimer systems. *Chem. Soc. Rev.* **44**, 3900–3923 (2015).
32. X. Yan, B. Jiang, T. R. Cook, Y. Zhang, J. Li, Y. Yu, F. Huang, H.-B. Yang, P. J. Stang, Dendronized organoplatinum(II) metallacyclic polymers constructed by hierarchical coordination-driven self-assembly and hydrogen-bonding interfaces. *J. Am. Chem. Soc.* **135**, 16813–16816 (2013).
33. M. Soler, G. R. Newkome, Supramolecular dendrimer chemistry, in *Supramolecular Chemistry: From Molecules to Nanomaterials*, J. W. Steed, P. A. Gale, Eds. (John Wiley & Sons, 2012).
34. A. Ciferri, Supramolecular polymerizations. *Macromol. Rapid Comm.* **23**, 511–529 (2002).
35. J. B. Beck, J. M. Ineman, S. J. Rowan, Metal/ligand-induced formation of metallo-supramolecular polymers. *Macromolecules* **38**, 5060–5068 (2005).
36. P. D. Frischmann, S. Guieu, R. Tabeshi, M. J. MacLachlan, Columnar organization of head-to-tail self-assembled Pt_4 rings. *J. Am. Chem. Soc.* **132**, 7668–7675 (2010).
37. W.-Y. Yang, E. Lee, M. Lee, Tubular organization with coiled ribbon from amphiphilic rigid-flexible macrocycle. *J. Am. Chem. Soc.* **128**, 3484–3485 (2006).
38. B.-S. Kim, D.-J. Hong, J. Bae, M. Lee, Controlled self-assembly of carbohydrate conjugate rod-coil amphiphiles for supramolecular multivalent ligands. *J. Am. Chem. Soc.* **127**, 16333–16337 (2005).
39. J.-H. Ryu, E. Lee, Y.-b. Lim, M. Lee, Carbohydrate-coated supramolecular structures: Transformation of nanofibers into spherical micelles triggered by guest encapsulation. *J. Am. Chem. Soc.* **129**, 4808–4814 (2007).
40. W. Burchard, Static and dynamic light scattering from branched polymers and biopolymers, in *Advances in Polymer Science* (Springer, 1983).
41. M. O. Blunt, J. C. Russell, M. d. C. Gimenez-Lopez, N. Taleb, X. Lin, M. Schröder, N. R. Champness, P. H. Beton, Guest-induced growth of a surface-based supramolecular bilayer. *Nat. Chem.* **3**, 74–78 (2011).
42. A. Ciesielski, A. Cadeddu, C.-A. Palma, A. Gorczyński, V. Patroniak, M. Cecchini, P. Samorì, Self-templating 2D supramolecular networks: A new avenue to reach control over a bilayer formation. *Nanoscale* **3**, 4125–4129 (2011).
43. H. Ozawa, M. Kawao, S. Uno, K. Nakazato, Preparation of various supramolecular assemblies and measurement of photoresponse behaviors. *Jpn. J. Appl. Phys.* **49**, 01AF05 (2010).
44. R. Wakabayashi, Y. Kubo, K. Kaneko, M. Takeuchi, S. Shinkai, Olefin metathesis of the aligned assemblies of conjugated polymers constructed through supramolecular bundling. *J. Am. Chem. Soc.* **128**, 8744–8745 (2006).
45. K. Takanashi, H. Chiba, M. Higuchi, K. Yamamoto, Efficient synthesis of poly(phenylazomethine) dendrons allowing access to higher generation dendrimers. *Org. Lett.* **6**, 1709–1712 (2004).
46. M. J. Frisch, G. W. Trucks, H. B. Schlegel, G. E. Scuseria, M. A. Robb, J. R. Cheeseman, G. Scalmani, V. Barone, B. Mennucci, G. A. Petersson, H. Nakatsuji, M. Caricato, X. Li, H. P. Hratchian, A. F. Izmaylov, J. Bloino, G. Zheng, J. L. Sonnenberg, M. Hada, M. Ehara, K. Toyota, R. Fukuda, J. Hasegawa, M. Ishida, T. Nakajima, Y. Honda, O. Kitao, H. Nakai, T. Vreven, J. A. Montgomery Jr., J. E. Peralta, F. Ogliaro, M. Bearpark, J. J. Heyd, E. Brothers, K. N. Kudin, V. N. Staroverov, R. Kobayashi, J. Normand, K. Raghavachari, A. Rendell, J. C. Burant, S. S. Iyengar, J. Tomasi, M. Cossi, N. Rega, J. M. Millam, M. Klene, J. E. Knox, J. B. Cross, V. Bakken, C. Adamo, J. Jaramillo, R. Gomperts, R. E. Stratmann, O. Yazyev, A. J. Austin, R. Cammi, C. Pomelli, J. W. Ochterski, R. L. Martin, K. Morokuma, V. G. Zakrzewski, G. A. Voth, P. Salvador, J. J. Dannenberg, S. Dapprich, A. D. Daniels, Ö. Farkas, J. B. Foresman, J. V. Ortiz, J. Cioslowski, D. J. Fox, *Gaussian 09 Revision C.01* (Gaussian Inc., 2009).

Acknowledgments

Funding: This study was supported, in part, by the Exploratory Research for Advanced Technology program of the Japan Science and Technology Agency; the MEXT Elements Strategy Initiative to Form Core Research Center, Japan; the Brain Korea 21 Plus program; the Basic Science Research program (NRF-2014R1A6A1030419); the Grant-in-Aid for Scientific Research on Innovative Areas, "pai-System figuration: Control of electron and structural dynamism for innovative functions"; and the Japan Society for the Promotion of Science KAKENHI grants 26410128, 15H00989, and 15H05757. **Author contributions:** Y.H., M.O., S.M., and Y.T. performed the experiments. K.A. performed the calculations. Y.A. and Y.M. helped and supervised the STM measurement. K.A. conceived the project. K.A. and K.Y. supervised the work, discussed the concept, and wrote the manuscript. **Competing interests:** The authors declare that they have no competing interests. **Data and materials availability:** All data needed to evaluate the conclusions in the paper are present in the paper and/or the Supplementary Materials. Additional data related to this paper may be requested from the authors.

Submitted 21 June 2016
Accepted 20 October 2016
Published 2 December 2016
10.1126/sciadv.1601414

Citation: K. Albrecht, Y. Hirabayashi, M. Otake, S. Mendori, Y. Tobari, Y. Azuma, Y. Majima, K. Yamamoto, Polymerization of a divalent/tetravalent metal-storing atom-mimicking dendrimer. *Sci. Adv.* **2**, e1601414 (2016).